Original Article

SLC12A8 upregulation promotes colorectal cancer progression and chemoresistance

Zhe Sun[1#], Zhiyan Nie[1#], Yao Xu[2#], Yingshun Cui[3], Wenjian Ma[1,4], Tongcun Zhang[1,2]

[1]College of Biotechnology, Tianjin University of Science and Technology, Tianjin, China; [2]Institute of Biology and Medicine, College of Life Sciences and Health, Wuhan University of Science and Technology, Wuhan, China; [3]Wuhan Tacro Technology Co., Ltd., Wuhan, China; [4]Qilu Institute of Technology, Jinan, China

Contributions: (I) Conception and design: Z Sun, Z Nie; (II) Administrative support: W Ma, T Zhang; (III) Provision of study materials or patients: Y Xu; (IV) Collection and assembly of data: Z Sun, Z Nie; (V) Data analysis and interpretation: Z Sun, Y Cui; (VI) Manuscript writing: All authors; (VII) Final approval of manuscript: All authors.

[#]These authors contributed equally to this work.

Correspondence to: Wenjian Ma, PhD. College of Biotechnology, Tianjin University of Science and Technology, #29 the 13th Avenue, TEDA, Tianjin 300457, China; Qilu Institute of Technology, Jinan, China. Email: ma_wj@tust.edu.cn; Tongcun Zhang, PhD. College of Biotechnology, Tianjin University of Science and Technology, #29 the 13th Avenue, TEDA, Tianjin 300457, China; Institute of Biology and Medicine, College of Life Sciences and Health, Wuhan University of Science and Technology, Wuhan, China. Email: zhangtongcun@wust.edu.cn.

Background: Colorectal cancer (CRC), a prevalent gastrointestinal malignant disease, causes substantial morbidity and mortality. Identification of novel prognostic biomarkers and therapeutic targets is critically needed to improve patient outcomes. Although solute carrier family 12 member 8 (SLC12A8) has high expression in various tumors and affects tumor progression, its role in CRC remains unclear. The aim of this study was to investigate the functions of SLC12A8 in CRC.

Methods: SLC12A8 expression and its association with clinical significance in CRC patients were explored via multiple public databases, including The Cancer Genome Atlas (TCGA), Genotype-Tissue Expression (GTEx), The Human Protein Atlas (HPA), The University of ALabama at Birmingham CANcer data analysis Portal (UALCAN), and Kaplan-Meier plotter. The effects of SLC12A8 on the CRC cell apoptosis, epithelial-mesenchymal transition (EMT), reactive oxygen species (ROS) production, and sensitivity to oxaliplatin were verified by *in vitro* experiments.

Results: SLC12A8 expression was upregulated in CRC tissues compared with normal colorectal tissues. Furthermore, high expression of SLC12A8 was associated with poorer prognosis in CRC patients. Pathway enrichment analyses revealed SLC12A8 involvement in oxidative stress and transforming growth factor-beta (TGF-β) signaling. Experiments in CRC cells showed that SLC12A8 upregulation promoted apoptosis resistance, EMT, and inhibited ROS production. Moreover, SLC12A8 knockdown enhanced the sensitivity of CRC cells to oxaliplatin chemotherapy.

Conclusions: Our integrative analyses identify SLC12A8 as a candidate biomarker for CRC progression. Targeting SLC12A8 may improve patient responses to oxaliplatin-based treatment regimens.

Keywords: Solute carrier family 12 member 8 (SLC12A8); colorectal cancer (CRC); reactive oxygen species (ROS); oxaliplatin

Submitted Jan 12, 2024. Accepted for publication Jun 02, 2024. Published online Jul 24, 2024.
doi: 10.21037/tcr-24-87
View this article at: https://dx.doi.org/10.21037/tcr-24-87

Introduction

Colorectal cancer (CRC) is a highly aggressive intestinal malignancy and the second leading cause of cancer-related death worldwide (1,2). Despite progress in screening and treatment, the overall survival (OS) rate for CRC patients remains low due to late-stage diagnosis, high rates of metastasis and recurrence, and resistance to therapeutic drugs (3-5). Uncovering mechanisms underlying CRC progression and drug resistance is therefore critical to improve patient outcomes. Altered cellular metabolism is a hallmark of cancer cells, and targeting cancer cell metabolism has emerged as a potential therapeutic strategy (6). Nicotinamide adenine dinucleotide (NAD^+) is a fundamental metabolite essential for multiple oxidation-reduction (redox) reactions that maintain cellular homeostasis and energy production. Moreover, elevated levels of NAD+ in cancer cells are involved in various nonredox molecular processes, including DNA repair, inflammatory responses, and apoptosis (7). Additionally, several genes involved in NAD^+ metabolism, such as NAMPT (8), SIRT1 (9), and PARP1 (10), have been found to contribute to cancer cell resistance to chemotherapy. This highlights the potential of targeting aberrant NAD^+ metabolism pathways to improve the effectiveness of chemotherapy in CRC.

The solute carrier family 12 member 8 (SLC12A8) belongs to the SLC12 gene family, which consists of electroneutral cation-chloride coupled cotransporters. Expression of genes in this family can be found in various human tissues and plays roles in regulating cell volume, transepithelial ion movement, intracellular chloride ion concentration, and blood pressure regulation (11). SLC12A8 has been recently identified as a transporter of NAD+ precursor nicotinamide mononucleotide (NMN) (12), and implicated in several malignant tumors including breast cancer (13), lung cancer (14), and bladder cancer (15,16). However, its functional significance in CRC remains unknown.

In order to elucidate the significance of SLC12A8 in colorectal tumorigenesis and chemoresistance, here we carried out an integrative analysis combing bioinformatics mining of public databases and experimental examination in CRC cell line models. Specifically, we analyzed whether SLC12A8 expression is dysregulated in CRC specimens and correlated with clinical outcomes. Additionally, we performed functional assays to determine if SLC12A8 regulates properties such as apoptosis, epithelial-mesenchymal transition (EMT), reactive oxygen species (ROS) generation, and oxaliplatin sensitivity that may promote CRC progression and drug resistance. We present this article in accordance with the REMARK and MDAR reporting checklists (available at https://tcr.amegroups.com/article/view/10.21037/tcr-24-87/rc).

Highlight box

Key findings

- High expression of solute carrier family 12 member 8 (SLC12A8) was found to be significantly associated with colorectal cancer (CRC) and led to a poor prognosis for CRC patients.
- High expression of SLC12A8 correlates with apoptosis resistance, epithelial-mesenchymal transition (EMT), inhibition of reactive oxygen species (ROS) production, and oxaliplatin resistance in CRC cells.

What is known and what is new?

- SLC12A8 plays important roles in tumor progression of several malignant tumors, including breast cancer, lung cancer, and bladder cancer.
- We identified SLC12A8 as a candidate biomarker for CRC diagnosis and prognosis. Additionally, we explored the role of SLC12A8 in apoptosis resistance, EMT, ROS production, and oxaliplatin resistance in CRC.

What is the implication, and what should change now?

- SLC12A8 could be developed as a promising therapeutic target for CRC. Additional investigations are required to fully understand the underlying molecular mechanism of SLC12A8 signaling in CRC.

Methods

Data acquisition and expression analysis

We explored SLC12A8 messenger RNA (mRNA) expression profiles in human normal and cancer tissues with The Cancer Genome Atlas (TCGA) (17) and Genotype-Tissue Expression (GTEx) database (18). We acquired both raw RNA-sequencing data and corresponding clinical information of tumor tissues and adjacent tissues for 33 different types of cancer. Gene expression data were retrieved from 647 colon adenocarcinoma (COAD) and rectum adenocarcinoma (READ) patients along with 51 normal tissues from TCGA. Additionally, the SLC12A8 expression data were obtained from GSE21510 (https://www.ncbi.nlm.nih.gov/geo/query/acc.cgi?acc=GSE21510) (19) and GSE44076 (https://www.ncbi.nlm.nih.gov/geo/query/acc.cgi?acc=GSE44076) (20) datasets in the Gene Expression Omnibus (GEO) database to verify the SLC12A8 expression levels in CRC and normal tissues. The Human Protein Atlas (HPA) database (21) was applied to determine SLC12A8 protein

expression levels in normal tissues and CRC tissues through immunohistochemistry (IHC) staining. We also assessed SLC12A8 promoter methylation status in COAD and READ using The University of ALabama at Birmingham CANcer data analysis Portal (UALCAN) database (22). The study was conducted in accordance with the Declaration of Helsinki (as revised in 2013).

Diagnostic value analysis

To evaluate the diagnostic accuracy of SLC12A8, the receiver operating characteristic (ROC) curve analysis based on sensitivity and specificity was conducted using the "pROC" package. The area under the curve (AUC) was between 0.5 and 1.0. AUC in 0.5–0.7 showed a low accuracy, AUC in 0.7–0.9 showed a certain accuracy, and AUC above 0.9 showed a high accuracy.

Prognostic value analysis

Kaplan-Meier Plotter (23) was used for prognostic analyses of SLC12A8 mRNA expression in colon cancer. Patient samples were split into two groups based on SLC12A8 expression by using the "auto select best cutoff" option. The OS, recurrence-free survival (RFS), and post progression survival (PPS) were analyzed, and the hazard ratio (HR) with 95% confidence intervals (CI) and log rank P value were calculated.

Functional enrichment analysis

We explored the differential expression genes (DEGs) between low-and high- SLC12A8 expression groups in CRC using DESeq2 package (24). The volcano plot was drawn by the ggplot2 package with the threshold of $|\log_2(\text{fold change})| > 1.0$ and $P<0.05$. The co-expression genes of SLC12A8 were screened using limma package. We explored top 20 co-expressed genes positively and negatively correlated with SLC12A8 expression in heatmaps using Spearman's correlation coefficient. The ClusterProfiler package was utilized for Gene Ontology (GO) analysis comprising of biological processes (BP), cellular components (CC), and molecular functions (MF), as well as Kyoto Encyclopedia of Genes and Genomes (KEGG) analysis (25). The ggplot2 package was employed for visualization. Adjusted $P<0.05$ was considered to be statistically significant in the enrichment results.

Gene set enrichment analysis (GSEA)

We used ClusteProfiler R package to explore the functional and pathway differences between the two groups of different SLC12A8 expression (26). Enrichment results met the conditions of adjusted $P<0.05$ and false discovery rate (FDR) q-value <0.25 were defined to be statistically significant.

Protein-protein interaction (PPI) network

Gene Multiple Association Network Integration Algorithm (GeneMANIA) (27), and Search Tool for the Retrieval of Interacting Genes (STRING) (28) were used to explore proteins that interact with SLC12A8 and constructed PPI networks.

Relationship between SLC12A8 expression and NAD^+ metabolism-related genes

We conducted a search for the term "NAD^+ metabolism" in GeneCards database (29) in order to retrieve genes related to NAD^+ metabolism. Genes extracted from GeneCards with an association score >30 and genes related with NAD^+ metabolism acquired from STRING were selected for analysis. We then performed correlation analysis between SLC12A8 expression and the identified NAD^+ metabolism-related genes and presented in a heatmap.

Cell culture

Human benign colon cells (NCM460) and human colon cancer cell lines (HT29 and HCT116) were obtained from American Type Culture Collection (ATCC). The cells were cultured in RPMI 1640 culture medium supplemented with 10% fetal bovine serum (FBS) and 1% penicillin/streptomycin under 5% CO_2 at 37 ℃.

Quantitative reverse transcription polymerase chain reaction (qRT-PCR)

Cells were lysed by Trizol and total RNA isolated. RNA was reverse transcribed into complementary DNA (cDNA) using a M-MLV Reverse Transcriptase (Promega, WI, USA). The real time PCR analyses were performed using SYBR on a StepOne Plus Real Time PCR system (Applied Biosystems, CA, USA). For SLC12A8, the following primers were used: SLC12A8 forward 5'-GGTGGGCAGACGGGAGGCA-3' and SLC12A8

reverse 5'-AGCGAAGGGCCTCTCGAGTG-3'. For glyceraldehyde 3-phosphate dehydrogenase (GAPDH) the following primers were used: GAPDH forward 5'-CGAGATCCCTCCAAAATCAA-3' and GAPDH reverse: 5'-TTCACACCCATGACGAACAT-3'. The relative expression of SLC12A8 was normalized to the expression of GAPDH using the $2^{-\Delta\Delta Ct}$ method.

Western blot

Cells were homogenized in radio immunoprecipitation assay (RIPA) lysis buffer with 1% phenylmethanesulfonyl fluoride (PMSF) (Solarbio, Beijing, China). The proteins were analyzed by 12% sodium dodecyl sulfate-polyacrylamide gel electrophoresis (SDS-PAGE) and then electrotransferred onto 0.2 μm polyvinylidene fluoride (PVDF) membranes (Millipore, MA, USA), and blocked utilizing 5% skimmed milk. Afterwards, membranes were incubated with primary antibodies against the following: SLC12A8 (NovusBio, Littleton, CO, USA), Bax (Abcam, Cambridge, MA, USA), Bcl-2 (Abcam, Cambridge, MA, USA), E-cadherin (Abmart, Shanghai, China), N-cadherin (Abmart), Vimentin (Abmart), and GAPDH (Affinity, Shanghai, China). Subsequently, the membranes were incubated with dye-coupled secondary antibodies (IRDye 680RD goat anti-rabbit and IRDye 680RD goat anti-mouse from LI-COR Biosciences, Lincoln, NE, USA) for 1h at room temperature. Finally, membranes were scanned using Odyssey Quantitative Fluorescent Imaging System (LI-COR Biosciences).

RNA interference

Small interfering RNAs (siRNAs) targeting SLC12A8 and negative control siRNA, were provided by RiboBio (Guangzhou, China). HiPerFect Transfection Reagent (Qiagen, Hilden, Germany) was used for cells transfection according to the manufacturer's instructions. Protein and total RNA were extracted 48–96 h after transfection for further assays.

ROS measurement

ROS production was detected by Reactive Oxygen Species Assay Kit (Beyotime, Shanghai, China) according to the manufacturer's protocol. After various treatments, cells were washed with phosphate buffered solution (PBS) and incubated with serum-free medium containing with 2',7'-dichlorofluorescin diacetate (DCFH-DA) at 37 ℃ for 20 min. Then DCFH-DA was removed and washed with serum-free medium three times. Dichlorofluorescein (DCF) fluorescence distribution of cells was detected using fluorescence microscope analysis (Olympus Fluoview, Japan).

Cell viability assay

Cells were treated with oxaliplatin (40 μmol/L, AbMole, Houston, TX, USA) for 48 h for further assays. Cell viability was then determined by methylthiazolyldiphenyl tetrazolium bromide (MTT) assays. Briefly, cells cultured at 96-well plates were incubated in the culture medium containing MTT (5 mg/mL, Solarbio) and cultured for 4 h at 37 ℃. The culture medium was then removed and replaced with 150 μL dimethyl sulfoxide (DMSO), followed by additional 10 min of incubation at 37 ℃. The absorbance at 490 nm was read on a spectrophotometric plate reader (Synergy4, BioTek, USA).

Statistical analysis

All bioinformatic analyses were conducted using the R programming language (version 4.2.1) and R package ggplot2 (version 3.3.6). The expression of SLC12A8 was analyzed by Wilcoxon rank sum test in unpaired samples, and paired t test in paired samples. The correlation between quantitative variables was assessed using Spearman's correlation analysis. All experimental results were performed in triplicate. Statistical significance was represented by $P<0.05$ (*), $P<0.01$ (**), and $P<0.001$ (***).

Results

SLC12A8 is overexpressed across multiple cancer types including CRC

To investigate the expression patterns of SLC12A8 in different types of cancer, we conducted a pan-cancer analysis using mRNA expression data from TCGA database and GTEx database. Out of 33 tumor types, 22 demonstrated statistically significant SLC12A8 upregulation relative to normal tissue controls, including bladder urothelial carcinoma (BLCA), breast invasive carcinoma (BRCA), cervical squamous cell carcinoma and endocervical adenocarcinoma (CESC), cholangiocarcinoma (CHOL), colon adenocarcinoma (COAD), lymphoid neoplasm diffuse

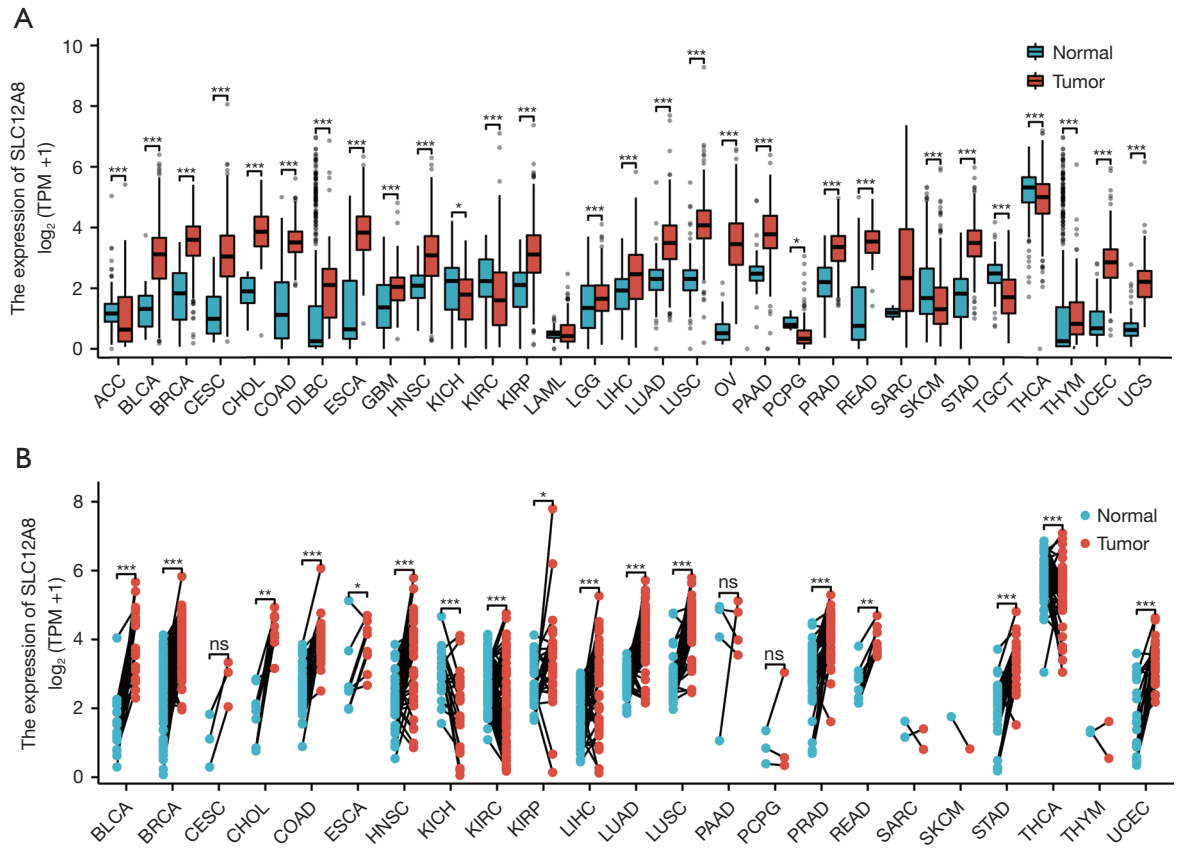

Figure 1 Expression status of SLC12A8 in pan-cancer. (A) Expression of SLC12A8 in TCGA cancers and normal tissues with the data of the GTEx database. (B) Expression of SLC12A8 in TCGA paired cancers and adjacent normal tissues. ns, P≥0.05; *, P<0.05; **, P<0.01; ***, P<0.001. SLC12A8, solute carrier family 12 member 8; TCGA, The Cancer Genome Atlas; GTEx, Genotype-Tissue Expression; TPM, transcripts per million; ACC, adrenocortical cancer; BLCA, bladder urothelial carcinoma; BRCA, breast cancer; CESC, cervical squamous cell carcinoma and endocervical adenocarcinoma; CHOL, cholangiocarcinoma; COAD, colon adenocarcinoma; DLBC, lymphoid neoplasm diffuse large B-cell lymphoma; ESCA, esophageal carcinoma; GBM, glioblastoma multiforme; HNSC, head and neck squamous cell carcinoma; KICH, kidney chromophobe; KIRC, kidney renal clear cell carcinoma; KIRP, kidney renal papillary cell carcinoma; LAML, acute myeloid leukemia; LGG, lower grade glioma; LIHC, liver hepatocellular carcinoma; LUAD, lung adenocarcinoma; LUSC, lung squamous cell carcinoma; OV, ovarian serous cystadenocarcinoma; PAAD, pancreatic adenocarcinoma; PCPG, pheochromocytoma and paraganglioma; PRAD, prostate adenocarcinoma; READ, rectal adenocarcinoma; SARC, sarcoma; SKCM, skin cutaneous melanoma; STAD, stomach adenocarcinoma; TGCT, testicular germ cell tumors; THCA, thyroid cancer; THYM, thymoma; UCEC, uterine corpus endometrioid cancer; UCS, uterine carcinosarcoma.

large B-cell lymphoma (DLBC), esophageal carcinoma (ESCA), glioblastoma multiforme (GBM), head and neck squamous cell carcinoma (HNSC), kidney renal papillary cell carcinoma (KIRP), lower grade glioma (LGG), liver hepatocellular carcinoma (LIHC), lung adenocarcinoma (LUAD), lung squamous cell carcinoma (LUSC), ovarian serous cystadenocarcinoma (OV), pancreatic adenocarcinoma (PAAD), prostate adenocarcinoma (PRAD), rectum adenocarcinoma (READ), stomach adenocarcinoma (STAD), thymoma (THYM), uterine corpus endometrial carcinoma (UCEC), and uterine carcinosarcoma (UCS) (*Figure 1A*). Mesothelioma (MESO) and uveal melanoma (UVM) could not be analyzed due to the lack of sufficient normal samples. Furthermore, comparison of 14 matched tumor and adjacent normal tissues revealed consistent SLC12A8 overexpression in cancerous tissues (*Figure 1B*).

After observing SLC12A8 overexpression profile across multiple cancers, we focused our analysis on CRC

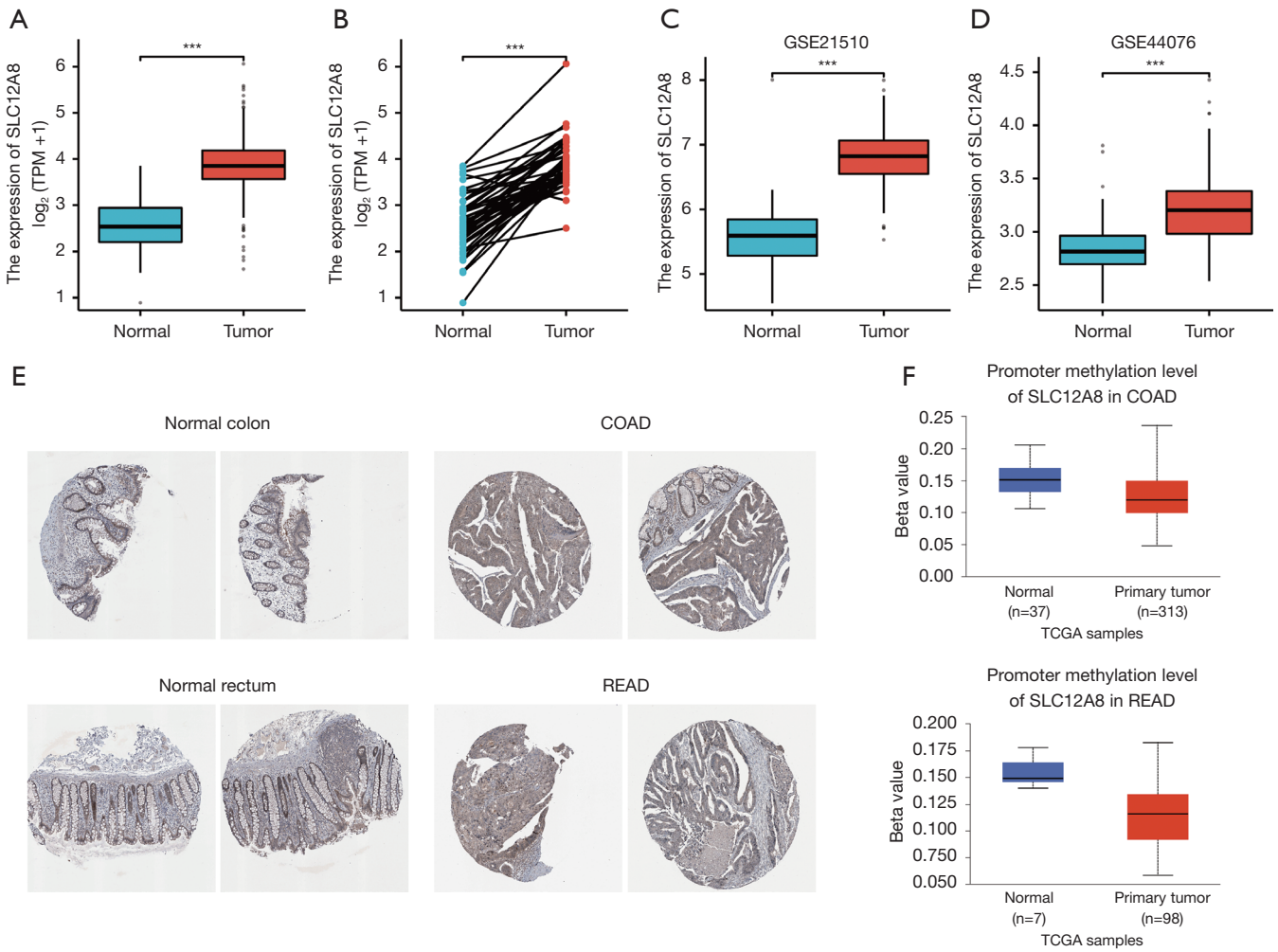

Figure 2 SLC12A8 expression in CRC patients. (A,B) Expression of SLC12A8 in CRC tissues and adjacent normal tissues according to the TCGA database. (C,D) Expression of SLC12A8 in CRC tissues and normal tissues according to the GEO database. (E) SLC12A8 protein expression by immunohistochemistry in CRC tissues and normal tissues (×200) based on HPA database. Normal tissue images are available from https://www.proteinatlas.org/ENSG00000221955-SLC12A8/tissue/colon#imid_7773246 (colon); https://www.proteinatlas.org/ENSG00000221955-SLC12A8/tissue/rectum (rectum). CRC tumor tissue images are available from https://www.proteinatlas.org/ENSG00000221955-SLC12A8/pathology/colorectal+cancer. (F) The promoter methylation levels of SLC12A8 in COAD and READ patients based on UALCAN database. ***, P<0.001. SLC12A8, solute carrier family 12 member 8; TPM, transcripts per million; TCGA, The Cancer Genome Atlas; GEO, Gene Expression Omnibus; HPA, The Human Protein Atlas; UALCAN, The University of ALabama at Birmingham CANcer data analysis Portal; CRC, colorectal cancer; COAD, colon adenocarcinoma; READ, rectal adenocarcinoma.

specifically. By utilizing TCGA data, we discovered that SLC12A8 was significantly upregulated in 647 CRC tumor samples versus 51 healthy colon controls (*Figure 2A*). This was further validated in an independent cohort of 50 paired patient-derived CRC and adjacent normal tissues (*Figure 2B*). In order to strengthen our findings, we also analyzed two additional CRC datasets from the GSE21510 and GSE44076 of the GEO database. Consistently, both datasets revealed higher levels of SLC12A8 expression in CRC patients (*Figure 2C,2D*). Lastly, higher SLC12A8 protein expression was detected in CRC tumors through analysis of HPA database (*Figure 2E*). To further explore the aberrant upregulated expression of SLC12A8 in CRC, we assessed the methylation status of SLC12A8 in CRC through UALCAN databases. The result displayed that the methylation levels of SLC12A8 promoter was lower in both

Table 1 Clinical characteristics of CRC patients

Characteristics	Low expression of SLC12A8 (n=322)	High expression of SLC12A8 (n=322)	P value
Pathologic T stage, n (%)			0.79
T1 & T2	62 (9.7)	69 (10.8)	
T3	220 (34.3)	216 (33.7)	
T4	38 (5.9)	36 (5.6)	
Pathologic N stage, n (%)			0.74
N0	179 (28)	189 (29.5)	
N1	80 (12.5)	73 (11.4)	
N2	60 (9.4)	59 (9.2)	
Pathologic M stage, n (%)			0.72
M0	241 (42.7)	234 (41.5)	
M1	47 (8.3)	42 (7.4)	
Pathologic stage, n (%)			0.84
Stage I	52 (8.3)	59 (9.5)	
Stage II	118 (18.9)	120 (19.3)	
Stage III	95 (15.2)	89 (14.3)	
Stage IV	47 (7.5)	43 (6.9)	
Age, n (%)			0.20
≤65 years	130 (20.2)	146 (22.7)	
>65 years	192 (29.8)	176 (27.3)	
Gender, n (%)			0.38
Female	145 (22.5)	156 (24.2)	
Male	177 (27.5)	166 (25.8)	

SLC12A8, solute carrier family 12 member 8; CRC, colorectal cancer; T, tumor; N, node; M, metastasis.

COAD and READ samples compared to normal samples (*Figure 2F*).

Association between SLC12A8 expression and clinicopathological characteristics in CRC

To elucidate connections between SLC12A8 expression and clinicopathological features in CRC, we evaluated the data of 644 CRC patients from the TCGA database. The patients were categorized into low and high SLC12A8 expression groups as shown in *Table 1*. Comparative analysis revealed that SLC12A8 expression was elevated across various pathological stages, tumor, node, metastasis (TNM) stages, and lymphatic invasion statuses compared to normal tissues (*Figure 3A-3E*). However, within the tumor tissues of COAD patients, SLC12A8 expression is relatively stable among the aforementioned clinicopathological features. These findings suggest a potential value of SLC12A8 in the early diagnosis of COAD. Interestingly, a high level of SLC12A8 mRNA expression was positively correlated with specific histological subtypes (*Figure 3F*), suggesting a connection with more aggressive disease characteristics.

SLC12A8 overexpression associates with poorer survival and serves as a diagnostic indicator in CRC

We assessed the prognostic value of SLC12A8 in CRC with Kaplan-Meier analysis. The results showed that increased SLC12A8 expression was strongly associated with adverse survival in CRC, including OS (*Figure 4A*), RFS (*Figure 4B*), and post-progression survival (PPS) (*Figure 4C*). These data indicate SLC12A8 expression levels hold prognostic utility for predicting clinical outcomes. To further evaluate its diagnosis value, we analyzed the SLC12A8 expression data of 698 CRC and normal tissue samples from TCGA using ROC curve analysis. The AUC was 0.939 (95% CI: 0.906–0.972) (*Figure 4D*), indicating excellent sensitivity and specificity profile as a diagnostic biomarker. These results suggest that SLC12A8 overexpression as both a prognostic indicator of poor CRC patient survival and an accurate diagnostic biomarker for colorectal malignancies.

SLC12A8 expression associates with pathways regulating chromatin architecture, cell death, and metabolism in CRC

To elucidate BP and pathways associated with SLC12A8 in CRC, gene expression profiling was performed on CRC specimens stratified by high and low SLC12A8 mRNA levels using TCGA datasets, which are based on the median SLC12A8 expression value using the criteria of $|\log_2 (\text{fold change})| > 1.0$ and $P<0.05$. Differential analysis identified 1,165 DEGs, with 88 genes showing up-regulation and 1,077 genes showing down-regulation (*Figure 5A*). To identify the genes that are most strongly correlated with SLC12A8 in COAD, we presented the top 20 genes that positively and negatively correlate with SLC12A8 expression in heatmaps (*Figure 5B,5C*).

The GO enrichment analysis of the identified DEGs revealed several intriguing biological themes related to chromatin assembly, apoptosis regulation, cell signaling

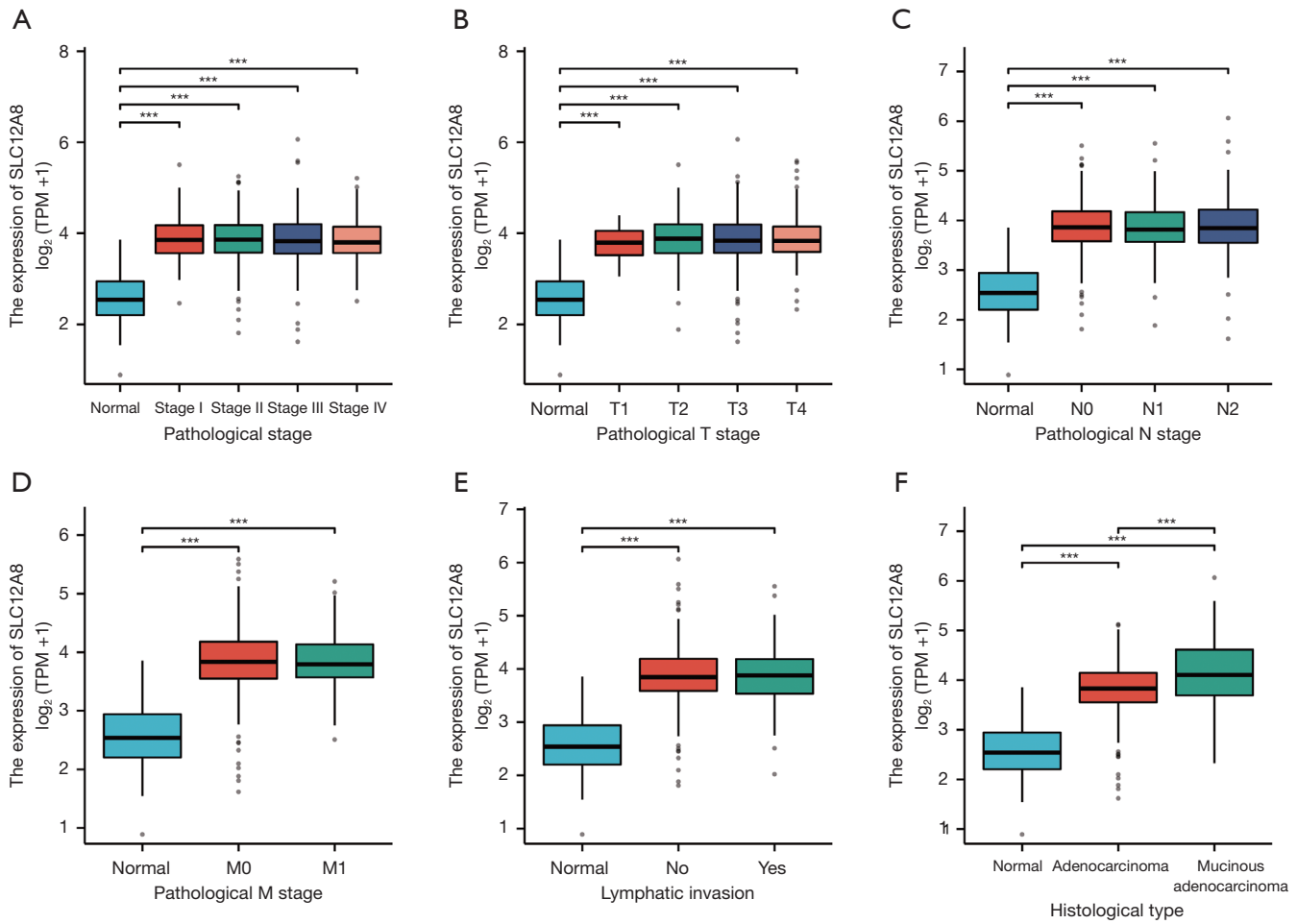

Figure 3 Correlation between SLC12A8 expression and clinical parameters in CRC patients. (A) Pathological stage, (B-D) TNM stage, (E) lymphatic invasion, (F) histological type. ***, P<0.001. SLC12A8, solute carrier family 12 member 8; TPM, transcripts per million; CRC, colorectal cancer; TNM, tumor, node, metastasis.

modulation, and metabolic pathways as shown in the bubble plot (*Figure 5D*). Notably, SLC12A8-correlated targets showed marked enrichment for nucleosome and protein-DNA complex organization, suggesting potential modulation of global chromatin architecture. The most enriched MF were protein heterodimerization activity, signaling receptor activation and inhibition, and receptor antagonist activity. Additionally, KEGG pathway analysis showed enrichment for neutrophil extracellular trap formation, peroxisome proliferator-activated receptor (PPAR) signaling pathway, cholesterol homeostasis, and nutrient metabolism emerged. The analysis implies SLC12A8 expression promotes CRC pathogenesis in part by eliciting epigenomic, cell death, and metabolic reprogramming.

SLC12A8 promotes extracellular matrix (ECM) remodeling, transforming growth factor-beta (TGF-β) signaling, and represses oxidative metabolism in CRC

In order to gain a broader understanding of the pathways regulated by SLC12A8 in CRC, we conducted GSEA analysis. GSEA based on the Reactome pathways indicated that SLC12A8-high tumors displayed marked enrichment for collagen formation, ECM proteoglycan, mesenchymal-epithelial transition (MET) factor activates protein tyrosine kinase 2 (PTK2) signaling, and integrin cell surface interactions (*Figure 6A*). Conversely, SLC12A8-low cancers showed significantly enriched pathways linked to oxidative stress-induced senescence, histone deacetylases (HDACs) deacetylate histones, DNA damage/telomere stress induced

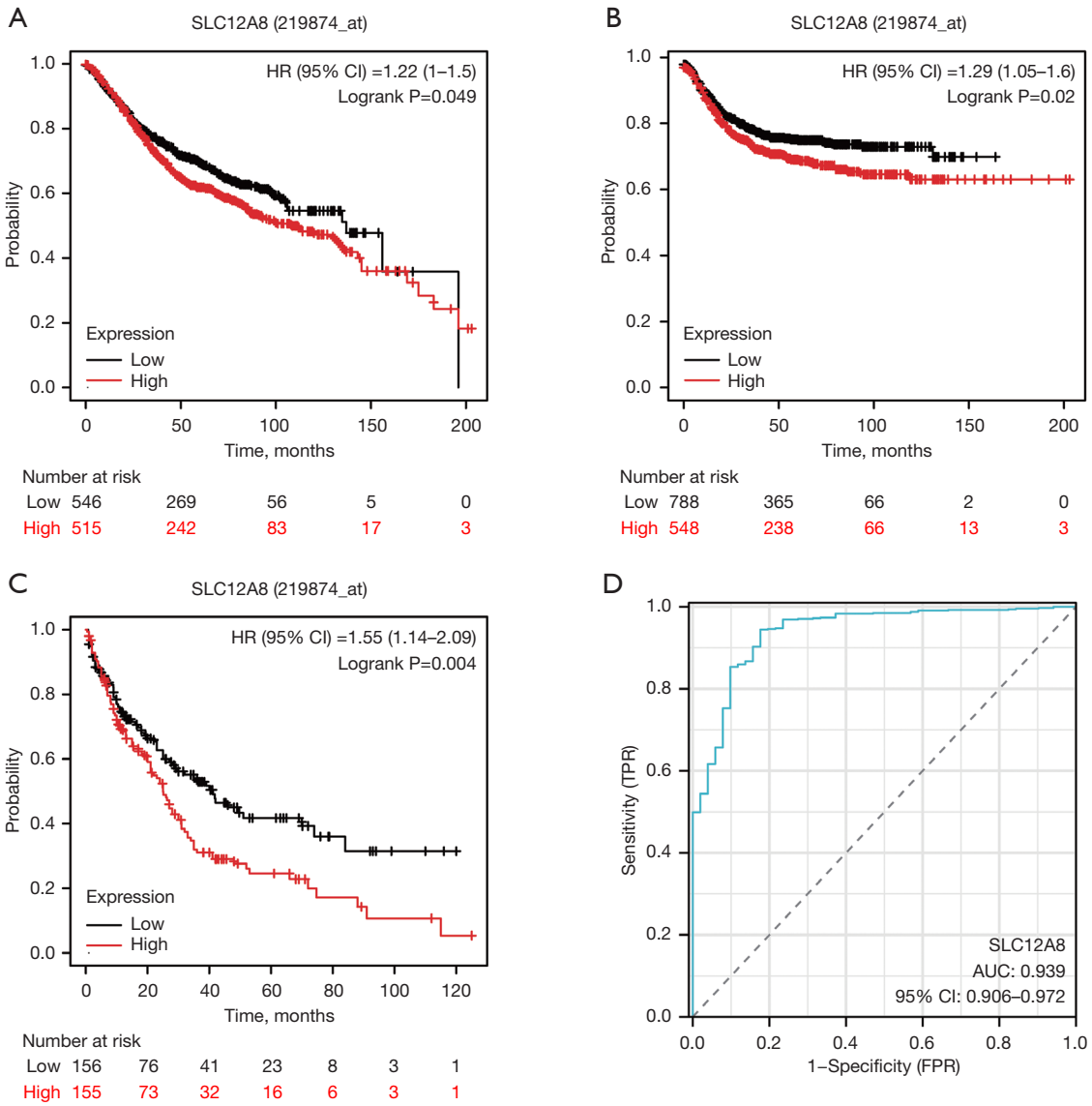

Figure 4 Prognostic and diagnostic value of SLC12A8 in CRC. (A-C) Kaplan-Meier survival curve analysis of OS, RFS and PPS in CRC cohort analyzed by Kaplan-Meier plotter database. (D) ROC curve of SLC12A8 expression in CRC cohort based on TCGA database. SLC12A8, solute carrier family 12 member 8; CRC, colorectal cancer; HR, hazard ratio; OS, overall survival; RFS, recurrence-free survival; PPS, post-progression survival; ROC, receiver operating characteristic; AUC, area under the curve; CI, confidence interval; TPR, true positive rate; FPR, false positive rate.

senescence, and DNA methylation (*Figure 6B*). Additionally, GSEA based on KEGG pathways revealed that pathways such as ECM-receptor-interaction, small cell lung cancer, TGF-β signaling pathway, and Fc gamma receptor-mediated phagocytosis were enriched in tumors with elevated SLC12A8 expression (*Figure 6C*). On the other hand, pathways involving ribosome, oxidative phosphorylation, systemic lupus erythematosus, and olfactory transduction were enriched in tumors with reduced SLC12A8 expression (*Figure 6D*). These GSEA results strongly suggest that SLC12A8 plays a role in regulating various BP relevant to CRC pathogenesis. Further studies validating and detailing these pathways mechanistically are warranted. Nonetheless, this integrative analysis provides valuable perspective into

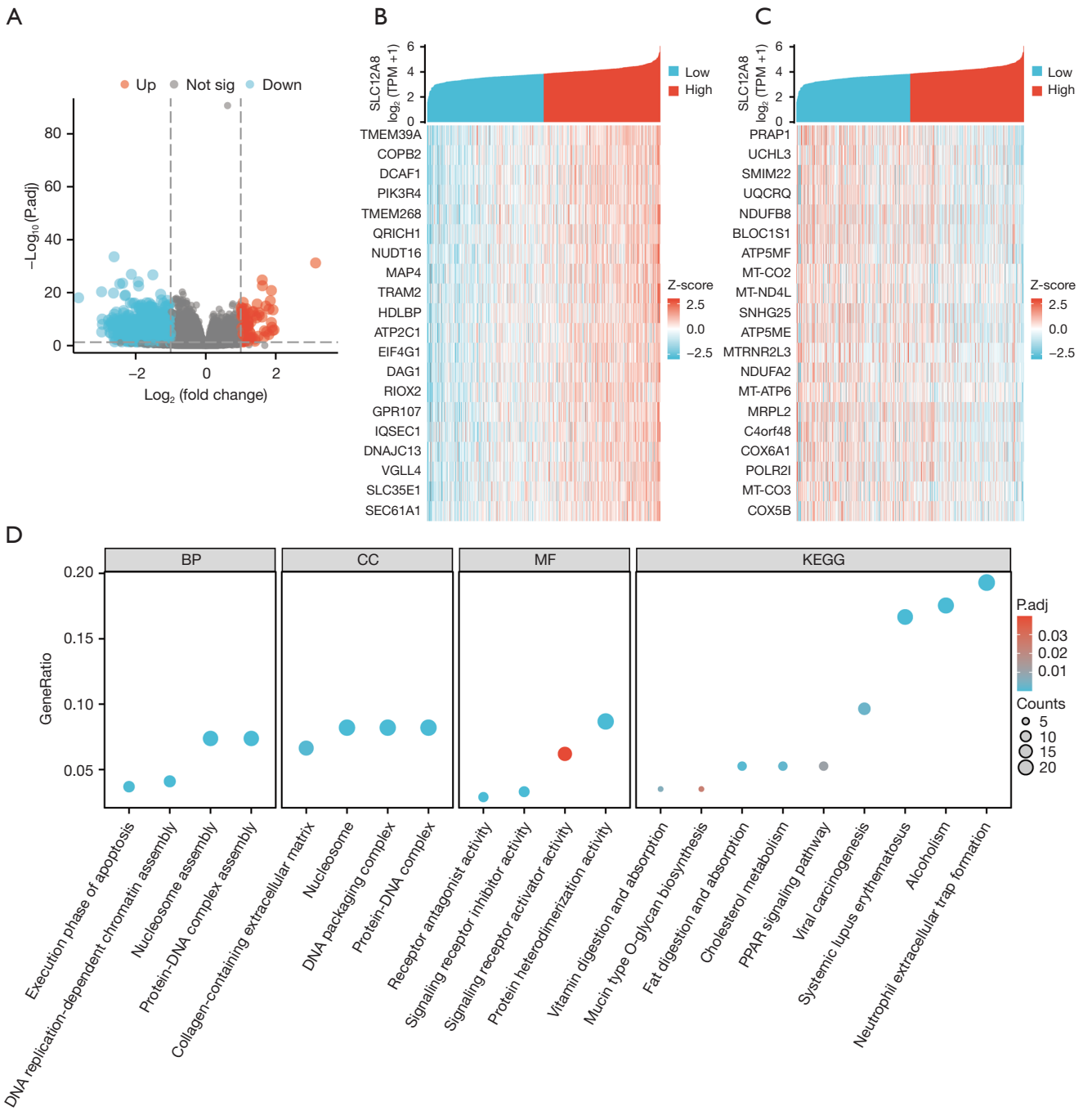

Figure 5 Functional enrichment analysis of SLC12A8 in CRC. (A) Volcano plot of differentially expressed genes between the high and low SLC12A8 expression groups. (B,C) Heat map showing the top 20 positively and negatively co-expressed genes with SLC12A8 in CRC. (D) GO and KEGG enrichment analysis of SLC12A8 expression-correlated DEGs. SLC12A8, solute carrier family 12 member 8; CRC, colorectal cancer; TPM, transcripts per million; GO, Gene Ontology; KEGG, Kyoto Encyclopedia of Genes and Genomes; BP, biological process; CC, cellular component; MF, molecular function; PPAR, peroxisome proliferator-activated receptor; DEGs, differential expression genes.

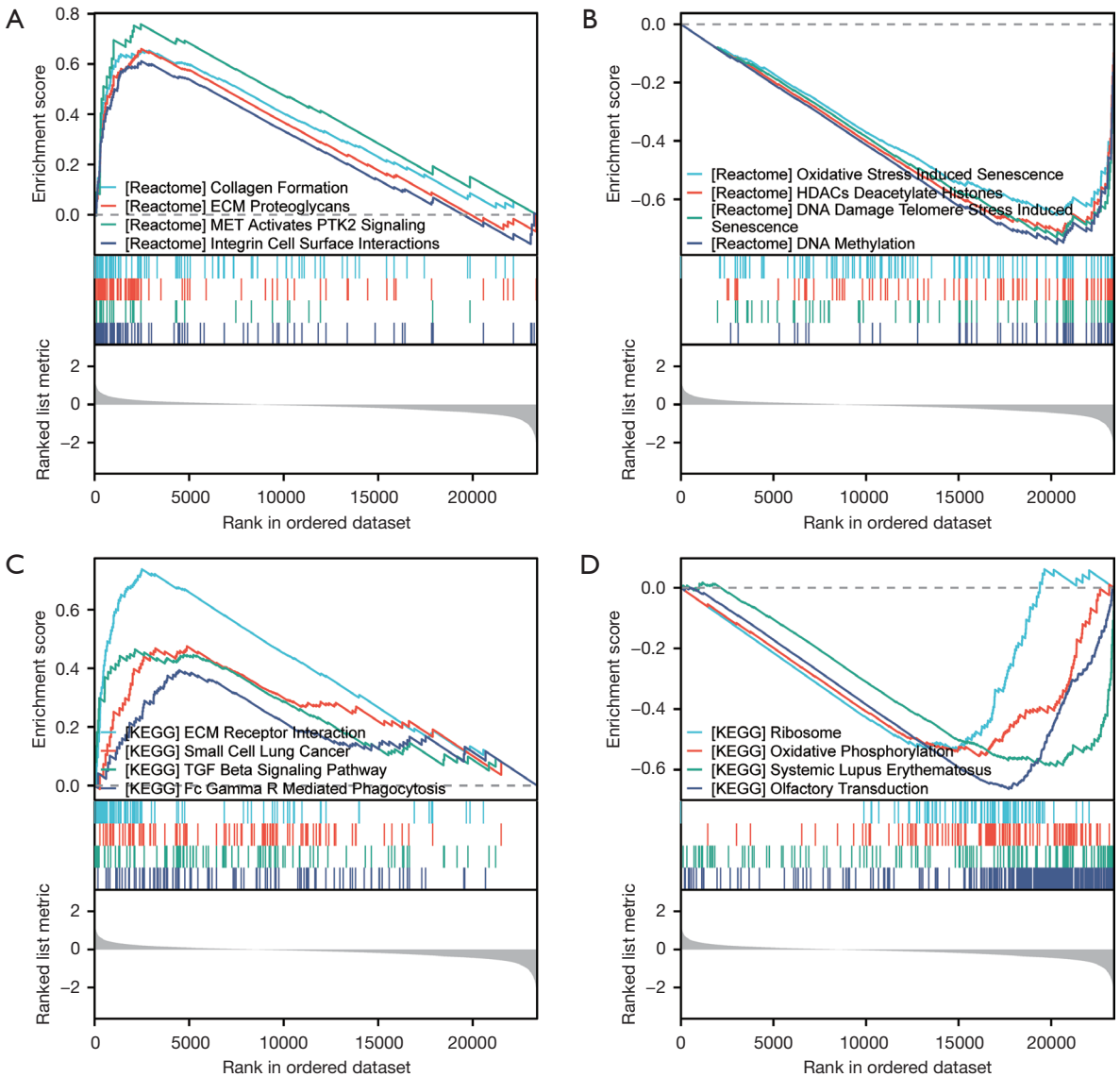

Figure 6 Enrichment plots from GSEA. (A,B) GSEA based on Reactome pathways. (C,D) GSEA based on KEGG pathways. GSEA, gene set enrichment analysis; KEGG, Kyoto Encyclopedia of Genes and Genomes; ECM, extracellular matrix; MET, mesenchymal-epithelial transition factor; PTK2, protein tyrosine kinase 2; HDACs, histone deacetylases; TGF, transforming growth factor.

the varied oncogenic processes influenced by SLC12A8 dysregulation to drive colorectal tumorigenesis.

SLC12A8 interacts with related SLC12 transporters and NAD⁺ metabolism genes in CRC

To gain further insights into the interacting partners and signaling networks involving SLC12A8 in CRC, we constructed PPI networks using GeneMANIA and STRING databases. Queried by GeneMANIA, SLC12A8 exhibited topological connections with other members of the SLC12 family involved in ion transport, including SLC12A7 and SLC12A9 (*Figure 7A*). STRING database analysis revealed additional links between SLC12A8 and multiple mediators of NAD^+ metabolism, including NMNAT1, NMNAT3, NAMPT, NMRK1, NAPRT, SLC25A51, and CD38 (*Figure 7B*). These results imply participation of SLC12A8 in coordinated ion transport processes and NAD+/NADP+ homeostatic pathways that may contribute to its oncogenic roles in CRC.

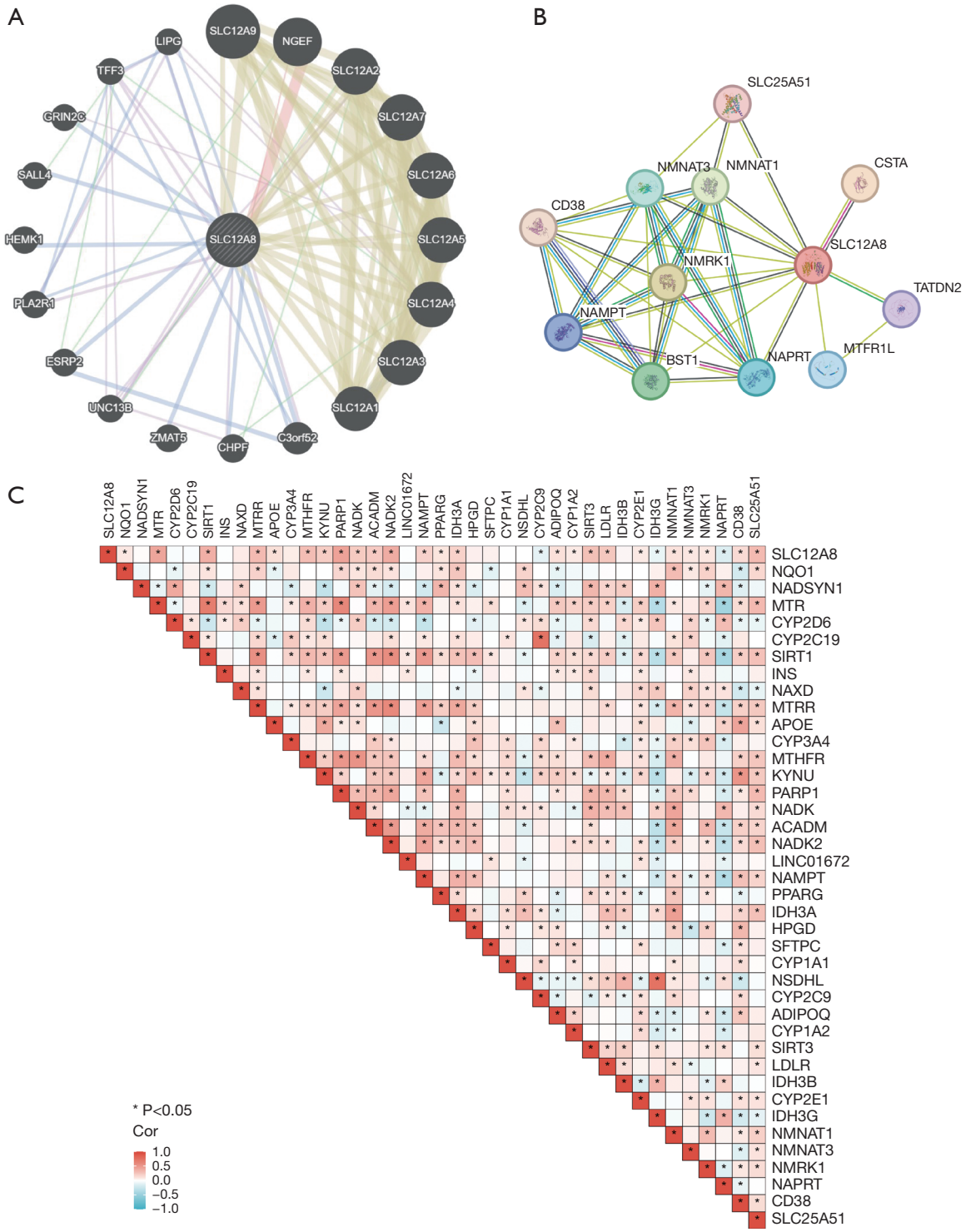

Figure 7 PPI network and correlation analysis of NAD+ metabolism-related genes. (A,B) The PPI network constructed on GeneMANIA database and STRING database. (C) Heatmap analysis of the correlation between SLC12A8 and NAD^+ metabolism-related genes in CRC. *, P<0.05. PPI, protein-protein interaction; SLC12A8, solute carrier family 12 member 8; CRC, colorectal cancer; NAD^+, nicotinamide adenine dinucleotide; GeneMANIA, Gene Multiple Association Network Integration Algorithm; STRING, Search Tool for the Retrieval of Interacting Genes.

In order to further understand the role of SLC12A8 in NAD^+ metabolism, we further evaluated the correlation between SLC12A8 and 39 NAD+ metabolism-related genes across CRC samples from TCGA. SLC12A8 levels showed significant positive correlations with multiple mediators governing NAD^+ biosynthesis (NAMPT, NMNAT1/3, NADK), consumption (SIRT1/3, PARPs), cellular import (SLC25A51), and related transcriptional programs (PPARG, PPARG targets) (*Figure 7C*, Figure S1). Negative correlations were conversely detected with select catabolic enzymes like NAPRT. These integrative findings confirm tight transcriptional linkage between SLC12A8 and critical control points regulating NAD^+ availability and flux in CRC cells. The coordinated upregulation of SLC12A8 with central NAD^+ metabolic regulators suggests its participation in sustaining the NAD^+ abundance required to maintain redox, signaling, and enzymatic processes necessary for sustained proliferation and survival.

SLC12A8 knockdown suppresses EMT and promotes apoptosis and oxidative stress in CRC

To further validate the above bioinformatic results, we performed wet experiments which confirmed that the expression of SLC12A8 mRNA and protein were both upregulated in human CRC cell lines (HT29 and HCT116) comparing to human benign colon cells (NCM460) (*Figure 8A*,*8B*). Loss-of-function studies were pursued through siRNA-mediated knockdown (*Figure 8C*,*8D*). SLC12A8 depletion resulted in increased expression of epithelial marker E-cadherin alongside decreased mesenchymal markers N-cadherin and vimentin (*Figure 8E*), indicative of impaired EMT, which is closely linked to tumor progression, metastasis, and drug resistance in CRC (30).

Bcl-2 and Bax are two key regulatory genes involved in apoptosis, with opposing functions. The ratio of Bcl-2/Bax is commonly used to monitor apoptosis. In this study, the groups with SLC12A8 knockdown showed decreased Bcl-2 protein expression and increased Bax protein expression (*Figure 8F*), shifting CRC cells towards apoptotic cell death. Moreover, we observed that SLC12A8 knockdown significantly increased production of ROS in CRC cells (*Figure 8G*), which play multiple roles in various signaling cascades associated with cell proliferation, transformation and cell death connecting to NAD+ metabolism (31). Collectively, these direct perturbation experiments suggest that SLC12A8 sustains CRC cell survival by stimulating EMT programming and suppressing apoptosis and oxidative stress pathways.

Knockdown of SLC12A8 enhances the sensitivity of colon cancer cells to oxaliplatin

Given links between SLC12A8, NAD+ metabolism and ROS production, we hypothesized SLC12A8-mediated redox changes may affect oxaliplatin responses. Supportively, colon cancer cells treated with oxaliplatin displayed a significant increase in ROS production compared to mock-treated control (Figure S2). Interestingly, a significant elevated expression of SLC12A8 protein was observed in oxaliplatin-treated colon cancer cells (*Figure 9A*). SLC12A8 knockdown exhibited a notable decrease in CRC cell viability following oxaliplatin treatment (*Figure 9B*). These findings imply SLC12A8 induction enables metabolic adaptations buffering against oxaliplatin cytotoxicity, possibly by reducing ROS production.

Discussion

Through mining large-scale bioinformatics resources and conducting functional experiments, here we demonstrate that SLC12A8 is upregulated in CRC, associating with poor prognosis. We further show SLC12A8 knockdown suppresses EMT, elevates apoptosis and ROS production, and enhance the sensitivity of CRC cells to oxaliplatin. Our findings identify SLC12A8 as a candidate prognostic biomarker, implying that targeting SLC12A8 could be a promising approach for overcoming oxaliplatin resistance in CRC patients.

SLC12A8 has been reported to play a role in NAD+ metabolism as an NMN transporter, allowing cells to meet the urgent demand for NAD+ synthesis (12). It was found that SLC12A8 has pro-tumor effects in various cancers and other neoplastic disease such as psoriasis (32). High expression of SLC12A8 has been linked to poorer prognosis in breast carcinoma, possibly due to its involvement in cell viability, invasiveness, and motility through the activation of the TLR/NLR signaling pathway (13). Another recent study reported that SLC12A8 is a predictive biomarker for poor prognosis in lung cancer and mediates TKI resistance through the PDK1/AKT axis (14).

Through analysis of the TCGA database, multiple GEO datasets, and the HPA database, the current study demonstrates that the expression of SLC12A8 in CRC

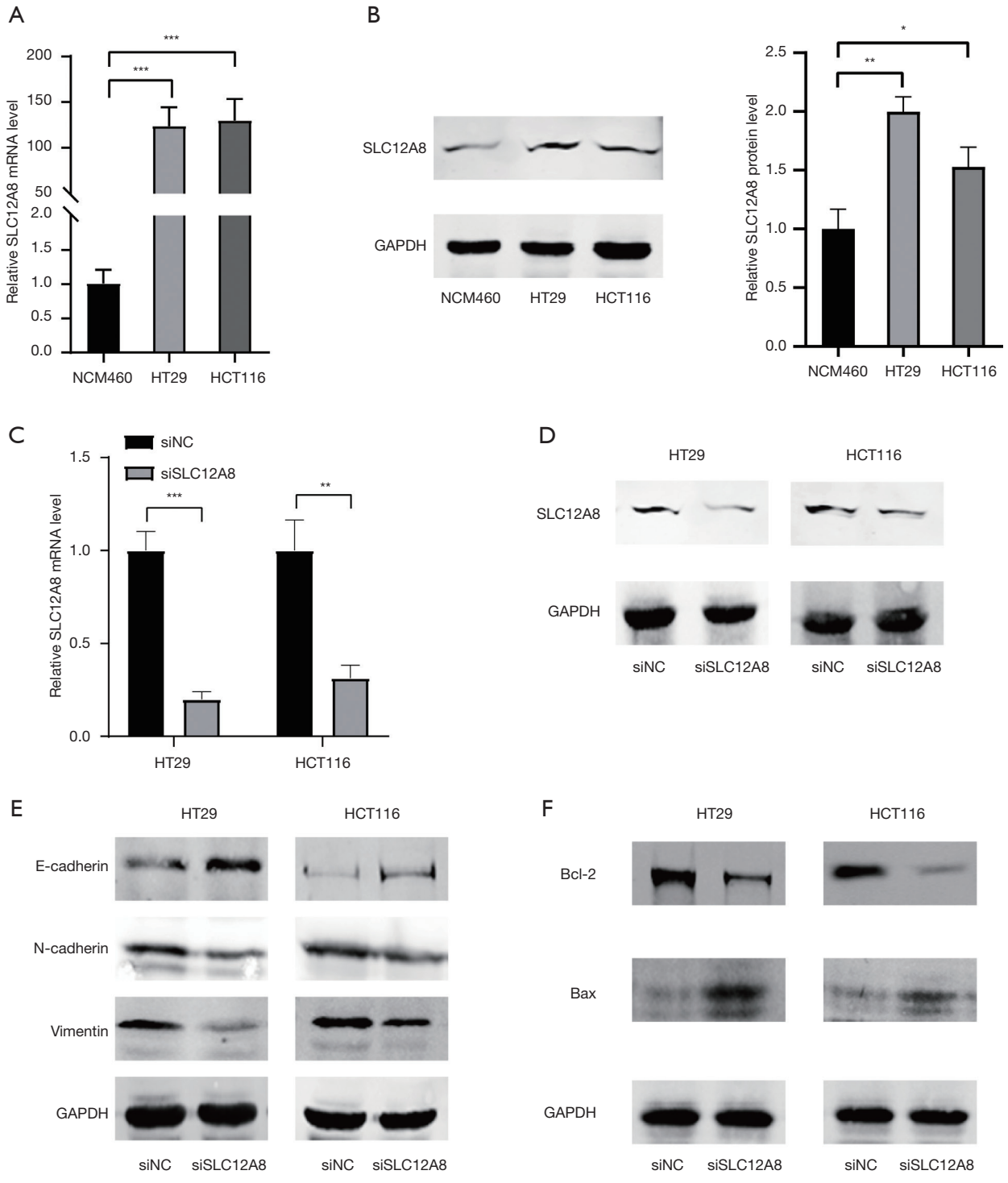

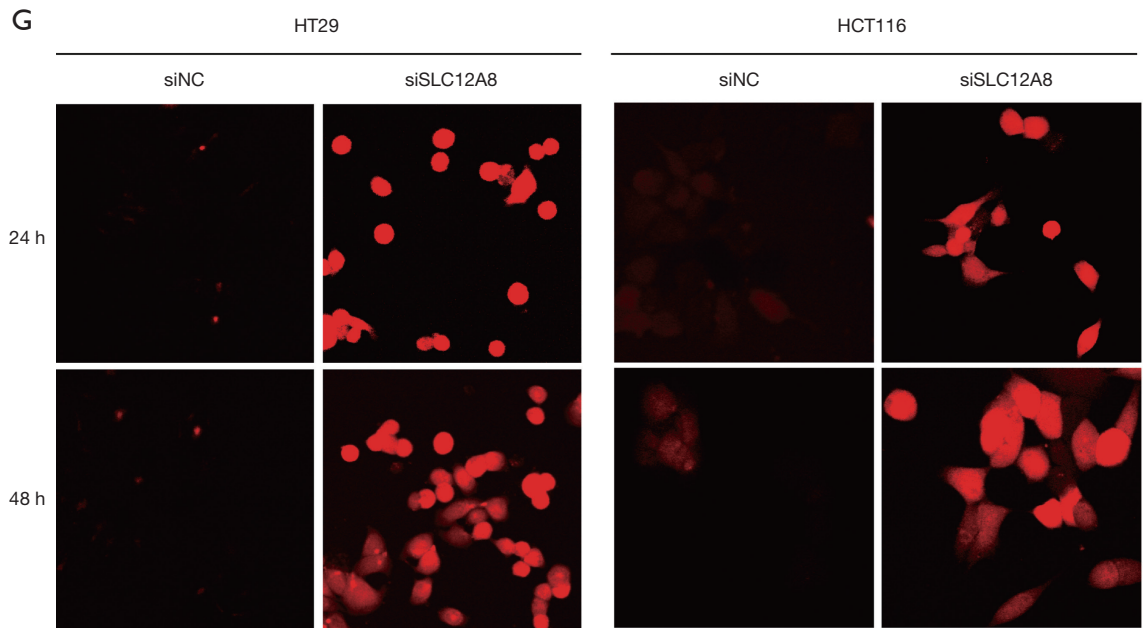

Figure 8 SLC12A8 knockdown inhibits epithelial-mesenchymal transition and promotes apoptosis and ROS production of CRC cells. (A) qRT-PCR analysis of SLC12A8 expression levels in normal colon epithelial cells (NCM460) and CRC cell lines (HT29 and HCT116). (B) Western blot analysis of SLC12A8 expression levels in NCM460, HT29, and HCT116 cells. (C) SLC12A8 knockdown efficiency in HT29 and HCT116 cells was analyzed by qRT-PCR. (D) SLC12A8 knockdown efficiency in HT29 and HCT116 cells was analyzed by Western blot. (E) Western blot analysis of E-cadherin, N-cadherin and Vimentin in HT29 and HCT116 cells with SLC12A8-siRNA transfection compared to negative control siRNA. (F) Western blot analysis of Bcl-2 and Bax in HT29 and HCT116 cells with SLC12A8-siRNA transfection compared to NC siRNA. (G) ROS production examined by DCF fluorescence microscopy (×400) was detected in HT29 and HCT116 cells with SLC12A8-siRNA transfection compared to NC siRNA. *, P<0.05; **, P<0.01; ***, P<0.001. SLC12A8, solute carrier family 12 member 8; GAPDH, glyceraldehyde-3-phosphate dehydrogenase; CRC, colorectal cancer; ROS, reactive oxygen species; siRNA, small interfering RNA; NC, negative control; DCF, dichlorofluorescein; qRT-PCR, quantitative reverse transcription polymerase chain reaction.

tissues is significantly higher than in normal tissues. Additionally, survival analysis and ROC curve analysis support SLC12A8 as a promising prognostic indicator and diagnostic biomarker for CRC. Beyond diagnostic and prognostic utility, our work suggests SLC12A8 inhibition may have therapeutic potential to restrain CRC growth and improve chemotherapeutic efficacy. By analyzing the top co-expressed genes with SLC12A8, we gain insights into its functional roles in CRC. Several genes closely associated with SLC12A8 have also been reported to promote the development of CRC. For example, COPB2, which is mainly found in the endoplasmic reticulum and Golgi stack membrane, is involved in intracellular protein transport and the development and progression of tumor cells (33). In CRC, silencing COPB2 can inhibit cell proliferation and induce apoptosis through the JNK/c-Jun signaling pathway (34). DCAF1, initially identified as a protein interacting with HIV-1 Vpr, is involved in cell cycle regulation and cell proliferation (35). Overexpression of DCAF1 has been reported in colon cancer and is associated with histone H2AT120 phosphorylation, leading to epigenetic gene inactivation and oncogenic transformation (36). PRAP1, a p53-responsive gene activated by genotoxic stress, has been found to promote oxaliplatin resistance in CRC by reducing ferroptosis (37). Another study revealed that overexpression of PRAP1 causes cisplatin resistance by inhibiting mitotic checkpoint complex assembly in CRC (38). The coordinated expression of these genes with SLC12A8 suggests their involvement in shared oncogenic programs that drive tumor progression. The GO and KEGG analyses and GSEA were conducted to thoroughly investigate the biological functions and potential mechanisms of SLC12A8 in the

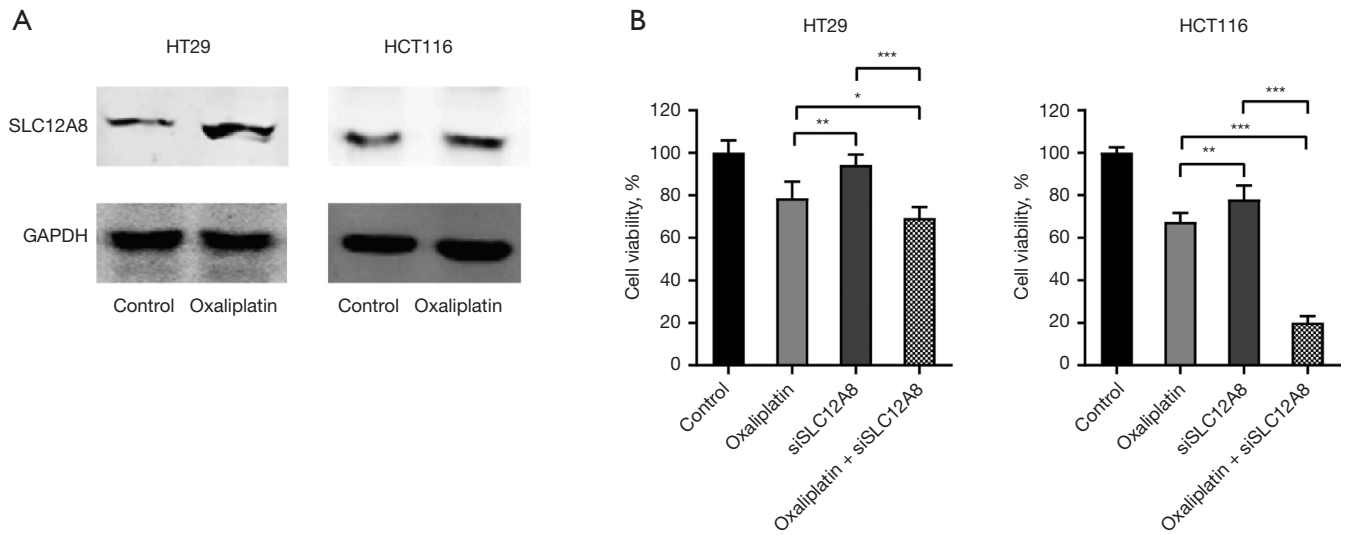

Figure 9 SLC12A8 knockdown enhances the sensitivity of CRC cells to oxaliplatin. (A) Western blot analysis of SLC12A8 protein expression in HT29 and HCT116 cells treated with or without oxaliplatin. (B) Cell viability was assessed by MTT assay to observe whether SLC12A8 knockdown would affect the lethal effect of oxaliplatin on HT29 and HCT116 cells. *, P<0.05; **, P<0.01; ***, P<0.001. SLC12A8, solute carrier family 12 member 8; GAPDH, glyceraldehyde-3-phosphate dehydrogenase; CRC, colorectal cancer; MTT, methylthiazolyldiphenyl tetrazolium bromide.

progression of CRC. The findings revealed significant associations between SLC12A8 and DNA packaging, signaling receptor activity, PPAR signaling pathway, ECM-receptor-interaction, TGF-β signaling pathway, oxidative stress, and DNA damage response. These associations indicate the potential mechanisms involved in SLC12A8-mediated carcinogenic processes in CRC. By mapping the PPI network for SLC12A8, we discovered close connections with genes involved in NAD^+ metabolism, such as NMNAT1, NAMPT, NAPRT, SLC25A51, and CD38. These genes have also been implicated in various human malignancies (39-41). Cancer cells have the ability to reprogram their metabolism to support rapid proliferation and survival under limited energy resources and adverse conditions (6). Cancer cells exhibit higher NAD^+/NADH and $NADP^+$/NADPH ratios compared to noncancerous cells, highlighting the importance of NAD^+ and NAD^+ metabolism-related genes in this metabolic alteration (42). We further investigated the correlation between SLC12A8 and NAD^+ metabolism-related genes in the TCGA-CRC dataset. The results demonstrated significant associations between SLC12A8 expression and several of these genes, highlighting the link between SLC12A8 and NAD^+ metabolism-related proteins in promoting cancer.

In vitro experiments confirmed the predicted oncogenic function of SLC12A8 in CRC by demonstrating upregulation of SLC12A8 in CRC cell lines. Additionally, knockdown of SLC12A8 in CRC cells led to weakened EMT, enhanced cell apoptosis, and increased ROS production. ROS production plays a crucial role in redox homeostasis and is vital for the survival of cancer cells. Furthermore, the anti-tumorigenic signaling of ROS can be targeted as a therapeutic approach, where increased ROS levels reach toxic levels and deplete the antioxidant system capacity, leading to programmed cell death and inhibition of EMT (43,44). Therefore, our results provide evidence supporting our hypothesis that SLC12A8 promotes CRC cell survival and EMT by inhibiting ROS production.

Tumor NAD+ metabolism and ROS production have been reported to play roles in promoting chemoresistance (45,46). Oxaliplatin, a third-generation platinum-based chemotherapeutic agent, has been clinically proven to combat a variety of malignancies, and is recommended as a first-line therapeutic regimen for metastatic CRC (47). It interacts with DNA to induce the formation of Pt-DNA adducts, subsequently resulting in cancer cell death (48). Unfortunately, intrinsic or acquired resistance to oxaliplatin based combinations still is the major cause of treatment failure (49). In this study, we demonstrated that SLC12A8 was upregulated in oxaliplatin treated CRC cells and

knockdown of SLC12A8 enhances the sensitivity of CRC cells to oxaliplatin. In addition, the differences in response between HT29 and HCT116 following simultaneous exposure to oxaliplatin combined with SLC12A8 knockdown may be attributed to the different genetic backgrounds of these cell lines. The HT29 cells have wild-type KRAS, while HCT116 cells carry the activating G13D mutation in KRAS (50). Many studies have reported the importance of NAD^+ metabolism in KRAS-mutated cancers (51,52). For this reason, NAD^+ is likely more important for the survival of HCT116 cells than for HT29 cells. Therefore, it would be of great interest to elucidate more detailed relationship between KRAS mutation and SLC12A8, which will support the rationale to explore new therapies such as inhibitors of NAD^+ biosynthesis as combinational therapy with oxaliplatin to prevent the development of oxaliplatin resistance.

Conclusions

In conclusion, we clarified the pro-cancer role of SLC12A8 in CRC from multiple perspectives. It is suggested that SLC12A8 can be used as a diagnostic and prognostic biomarker, and a promising therapeutic target for CRC. While compelling, additional investigations into the precise molecular underpinnings of SLC12A8 signaling are still needed. Furthermore, validation of its clinical utility as a biomarker using patient samples along with *in vivo* preclinical models evaluating therapeutic inhibition promise to provide more definitive evidence supporting translation of our findings. Overall, this work provides a strong foundation establishing SLC12A8 as a potential biomarker and chemotherapeutic target in CRC worthy of continued research.

Acknowledgments

Funding: This work was supported by the National Key R&D Program of China (No. 2018YFA0901702); the National Science Foundation of Shandong (No. ZR2022MC057); the Foundation of Hubei Province Supporting Enterprise Technology Innovation Development (No. 2021BAB126); and Wuhan East Lake High-tech Zone "JieBangGuaShuai" Project (No. 2022KJB113).

Footnote

Reporting Checklist: The authors have completed the REMARK and MDAR reporting checklists. Available at https://tcr.amegroups.com/article/view/10.21037/tcr-24-87/rc

Data Sharing Statement: Available at https://tcr.amegroups.com/article/view/10.21037/tcr-24-87/dss

Peer Review File: Available at https://tcr.amegroups.com/article/view/10.21037/tcr-24-87/prf

Conflicts of Interest: All authors have completed the ICMJE uniform disclosure form (available at https://tcr.amegroups.com/article/view/10.21037/tcr-24-87/coif). Y.C. is an employee of Wuhan Tacro Technology Co., Ltd. The other authors have no conflicts of interest to declare.

Ethical Statement: The authors are accountable for all aspects of the work in ensuring that questions related to the accuracy or integrity of any part of the work are appropriately investigated and resolved. The study was conducted in accordance with the Declaration of Helsinki (as revised in 2013).

References

1. Siegel RL, Giaquinto AN, Jemal A. Cancer statistics, 2024. CA Cancer J Clin 2024;74:12-49.
2. Sung H, Ferlay J, Siegel RL, et al. Global Cancer Statistics 2020: GLOBOCAN Estimates of Incidence and Mortality Worldwide for 36 Cancers in 185 Countries. CA Cancer J Clin 2021;71:209-49.
3. Shin AE, Giancotti FG, Rustgi AK. Metastatic colorectal cancer: mechanisms and emerging therapeutics. Trends Pharmacol Sci 2023;44:222-36.
4. Bando H, Ohtsu A, Yoshino T. Therapeutic landscape and future direction of metastatic colorectal cancer. Nat Rev Gastroenterol Hepatol 2023;20:306-22.
5. Ma SC, Zhang JQ, Yan TH, et al. Novel strategies to reverse chemoresistance in colorectal cancer. Cancer Med

2023;12:11073-96.
6. Hanahan D. Hallmarks of Cancer: New Dimensions. Cancer Discov 2022;12:31-46.
7. Navas LE, Carnero A. Nicotinamide Adenine Dinucleotide (NAD) Metabolism as a Relevant Target in Cancer. Cells 2022;11:2627.
8. Nacarelli T, Fukumoto T, Zundell JA, et al. NAMPT Inhibition Suppresses Cancer Stem-like Cells Associated with Therapy-Induced Senescence in Ovarian Cancer. Cancer Res 2020;80:890-900.
9. Wang XW, Jiang YH, Ye W, et al. SIRT1 promotes the progression and chemoresistance of colorectal cancer through the p53/miR-101/KPNA3 axis. Cancer Biol Ther 2023;24:2235770.
10. Pyndiah S, Tanida S, Ahmed KM, et al. c-MYC suppresses BIN1 to release poly(ADP-ribose) polymerase 1: a mechanism by which cancer cells acquire cisplatin resistance. Sci Signal 2011;4:ra19.
11. Hebert SC, Mount DB, Gamba G. Molecular physiology of cation-coupled Cl- cotransport: the SLC12 family. Pflugers Arch 2004;447:580-93.
12. Grozio A, Mills KF, Yoshino J, et al. Slc12a8 is a nicotinamide mononucleotide transporter. Nat Metab 2019;1:47-57.
13. Li L, Xia J, Cui R, et al. Solute carrier family 12 member 8 impacts the biological behaviors of breast carcinoma cells by activating TLR/NLR signaling pathway. Cytotechnology 2021;73:23-34.
14. Huang F, Cui J, Wan J, et al. SLC12A8 mediates TKI resistance in EGFR-mutant lung cancer via PDK1/AKT axis. J Cancer Res Clin Oncol 2023;149:16729-39.
15. Li SL, Li ZF, Cao QW, et al. SLC12A8 plays a key role in bladder cancer progression and EMT. Open Med (Wars) 2020;16:58-67.
16. Zhang Q, Liu Y, Chen P, et al. Solute carrier family 12 member 8 (SLC12A8) is a potential biomarker and related to tumor immune cell infiltration in bladder cancer. Bioengineered 2021;12:4946-61.
17. Tomczak K, Czerwińska P, Wiznerowicz M. The Cancer Genome Atlas (TCGA): an immeasurable source of knowledge. Contemp Oncol (Pozn) 2015;19:A68-77.
18. The GTEx Consortium atlas of genetic regulatory effects across human tissues. Science 2020;369:1318-30.
19. Tsukamoto S, Ishikawa T, Iida S, et al. Clinical significance of osteoprotegerin expression in human colorectal cancer. Clin Cancer Res 2011;17:2444-50.
20. Cordero D, Solé X, Crous-Bou M, et al. Large differences in global transcriptional regulatory programs of normal and tumor colon cells. BMC Cancer 2014;14:708.
21. Uhlén M, Fagerberg L, Hallström BM, et al. Proteomics. Tissue-based map of the human proteome. Science 2015;347:1260419.
22. Chandrashekar DS, Karthikeyan SK, Korla PK, et al. UALCAN: An update to the integrated cancer data analysis platform. Neoplasia 2022;25:18-27.
23. Kovács SA, Fekete JT, Győrffy B. Predictive biomarkers of immunotherapy response with pharmacological applications in solid tumors. Acta Pharmacol Sin 2023;44:1879-89.
24. Love MI, Huber W, Anders S. Moderated estimation of fold change and dispersion for RNA-seq data with DESeq2. Genome Biol 2014;15:550.
25. Yu G, Wang LG, Han Y, et al. clusterProfiler: an R package for comparing biological themes among gene clusters. OMICS 2012;16:284-7.
26. Subramanian A, Tamayo P, Mootha VK, et al. Gene set enrichment analysis: a knowledge-based approach for interpreting genome-wide expression profiles. Proc Natl Acad Sci U S A 2005;102:15545-50.
27. Warde-Farley D, Donaldson SL, Comes O, et al. The GeneMANIA prediction server: biological network integration for gene prioritization and predicting gene function. Nucleic Acids Res 2010;38:W214-20.
28. Szklarczyk D, Kirsch R, Koutrouli M, et al. The STRING database in 2023: protein-protein association networks and functional enrichment analyses for any sequenced genome of interest. Nucleic Acids Res 2023;51:D638-46.
29. Stelzer G, Rosen N, Plaschkes I, et al. The GeneCards Suite: From Gene Data Mining to Disease Genome Sequence Analyses. Curr Protoc Bioinformatics 2016;54:1.30.1-1.30.33.
30. Zhang N, Ng AS, Cai S, et al. Novel therapeutic strategies: targeting epithelial-mesenchymal transition in colorectal cancer. Lancet Oncol 2021;22:e358-68.
31. Sedlackova L, Korolchuk VI. The crosstalk of NAD, ROS and autophagy in cellular health and ageing. Biogerontology 2020;21:381-97.
32. Hüffmeier U, Lascorz J, Traupe H, et al. Systematic linkage disequilibrium analysis of SLC12A8 at PSORS5 confirms a role in susceptibility to psoriasis vulgaris. J Invest Dermatol 2005;125:906-12.
33. Feng Y, Lei X, Zhang L, et al. COPB2: a transport protein with multifaceted roles in cancer development and progression. Clin Transl Oncol 2021;23:2195-205.
34. Wang Y, Xie G, Li M, et al. COPB2 gene silencing inhibits colorectal cancer cell proliferation and induces

apoptosis via the JNK/c-Jun signaling pathway. PLoS One 2020;15:e0240106.
35. Le Rouzic E, Belaïdouni N, Estrabaud E, et al. HIV1 Vpr arrests the cell cycle by recruiting DCAF1/VprBP, a receptor of the Cul4-DDB1 ubiquitin ligase. Cell Cycle 2007;6:182-8.
36. Ghate NB, Kim S, Shin Y, et al. Phosphorylation and stabilization of EZH2 by DCAF1/VprBP trigger aberrant gene silencing in colon cancer. Nat Commun 2023;14:2140.
37. Zhang Q, Deng T, Zhang H, et al. Adipocyte-Derived Exosomal MTTP Suppresses Ferroptosis and Promotes Chemoresistance in Colorectal Cancer. Adv Sci (Weinh) 2022;9:e2203357.
38. Song J, Chen Y, Yu H, et al. Proline-rich acidic protein 1 upregulates mitotic arrest deficient 1 to promote cisplatin-resistance of colorectal carcinoma by restraining mitotic checkpoint complex assembly. J Cancer 2023;14:1515-30.
39. Kiss A, Csikos C, Regdon Z, et al. NMNAT1 Is a Survival Factor in Actinomycin D-Induced Osteosarcoma Cell Death. Int J Mol Sci 2021;22:8869.
40. Li Y, Bie J, Zhao L, et al. SLC25A51 promotes tumor growth through sustaining mitochondria acetylation homeostasis and proline biogenesis. Cell Death Differ 2023;30:1916-30.
41. Zeidler JD, Hogan KA, Agorrody G, et al. The CD38 glycohydrolase and the NAD sink: implications for pathological conditions. Am J Physiol Cell Physiol 2022;322:C521-45.
42. Navas LE, Carnero A. NAD(+) metabolism, stemness, the immune response, and cancer. Signal Transduct Target Ther 2021;6:2.
43. Zhao Y, Ye X, Xiong Z, et al. Cancer Metabolism: The Role of ROS in DNA Damage and Induction of Apoptosis in Cancer Cells. Metabolites 2023;13:796.
44. Lee JXT, Tan WR, Low ZS, et al. YWHAG Deficiency Disrupts the EMT-Associated Network to Induce Oxidative Cell Death and Prevent Metastasis. Adv Sci (Weinh) 2023;10:e2301714.
45. Nikas IP, Paschou SA, Ryu HS. The Role of Nicotinamide in Cancer Chemoprevention and Therapy. Biomolecules 2020;10:477.
46. Zhou X, An B, Lin Y, et al. Molecular mechanisms of ROS-modulated cancer chemoresistance and therapeutic strategies. Biomed Pharmacother 2023;165:115036.
47. Kim GP, Erlichman C. Oxaliplatin in the treatment of colorectal cancer. Expert Opin Drug Metab Toxicol 2007;3:281-94.
48. Raymond E, Faivre S, Woynarowski JM, et al. Oxaliplatin: mechanism of action and antineoplastic activity. Semin Oncol 1998;25:4-12.
49. Martinez-Balibrea E, Martínez-Cardús A, Ginés A, et al. Tumor-Related Molecular Mechanisms of Oxaliplatin Resistance. Mol Cancer Ther 2015;14:1767-76.
50. Bose D, Zimmerman LJ, Pierobon M, et al. Chemoresistant colorectal cancer cells and cancer stem cells mediate growth and survival of bystander cells. Br J Cancer 2011;105:1759-67.
51. Yau EH, Kummetha IR, Lichinchi G, et al. Genome-Wide CRISPR Screen for Essential Cell Growth Mediators in Mutant KRAS Colorectal Cancers. Cancer Res 2017;77:6330-9.
52. Sessions DT, Kim KB, Kashatus JA, et al. Opa1 and Drp1 reciprocally regulate cristae morphology, ETC function, and NAD(+) regeneration in KRas-mutant lung adenocarcinoma. Cell Rep 2022;41:111818.

Cite this article as: Sun Z, Nie Z, Xu Y, Cui Y, Ma W, Zhang T. SLC12A8 upregulation promotes colorectal cancer progression and chemoresistance. Transl Cancer Res 2024;13(7):3446-3464. doi: 10.21037/tcr-24-87

